ESC European Society of Cardiology

Cardiovascular Research (2019) **115**, 343–356
doi:10.1093/cvr/cvy207

Y-27632 preconditioning enhances transplantation of human-induced pluripotent stem cell-derived cardiomyocytes in myocardial infarction mice

Meng Zhao[1,2], Chengming Fan[2,3], Patrick J. Ernst[2,4], Yawen Tang[2], Hanxi Zhu[2], Saidulu Mattapally[2], Yasin Oduk[2], Anton V. Borovjagin[2], Lufang Zhou[2,4], Jianyi Zhang[2]*, and Wuqiang Zhu[2]*

[1]Department of Physiology and Pathophysiology, Shanghai Medical College, Fudan University, Shanghai, China; [2]Department of Biomedical Engineering, School of Medicine, School of Engineering, University of Alabama at Birmingham, 1670 University Blvd, VH G094E, Birmingham, AL 35233, USA; [3]Department of Cardiovascular Surgery, the Second Xiangya Hospital, Central South University, Changsha, China; and[4]Division of Cardiovascular Diseases, School of Medicine, University of Alabama at Birmingham, Birmingham, AL, USA

Received 5 January 2018; revised 20 April 2018; editorial decision 26 July 2018; accepted 10 August 2018; online publish-ahead-of-print 13 August 2018

Time for primary review: 48 days

Aims The effectiveness of cell-based treatments for regenerative myocardial therapy is limited by low rates of cell engraftment. Y-27632 inhibits Rho-associated protein kinase (ROCK), which regulates the cytoskeletal changes associated with cell adhesion, and has been used to protect cultured cells during their passaging. Here, we investigated whether preconditioning of cardiomyocytes, derived from human-induced pluripotent stem cells (hiPSC-CM), with Y-27632 improves their survival and engraftment in a murine model of acute myocardial infarction (MI).

Methods and results After MI induction, mice were subjected to intramyocardial injections of phosphate-buffered saline, hiPSC-CM cultured under standard conditions (hiPSC-CM^{-RI}), or Y-27632-preconditioned hiPSC-CM (hiPSC-CM^{+RI}). The resulting engraftment rate calculated 4 weeks after implantation was significantly higher and the abundance of apoptotic transplanted cells was significantly lower in hiPSC-CM^{+RI} recipients than in hiPSC-CM^{-RI} animals. In cultured hiPSC-CM, Y-27632-preconditioning reversibly reduced contractile activity and the expression of troponin genes, while increasing their attachment to an underlying mouse cardiomyocyte (HL1) monolayer. Y-27632 preconditioning also increased the expression of N-cadherin and integrin ß1, the two cell junction proteins. hiPSC-CM^{+RI} were also larger in cell area with greater cytoskeletal alignment and a more rod-like shape than hiPSC-CM^{-RI}, both after transplantation (*in vivo*) and in culture. The effects of Y-27632 preconditioning on contractile activity and morphology of hiPSC-CMs in culture, as well as on their engraftment rate and apoptotic death in MI mouse grafts, could be recapitulated by hiPSC-CM treatment with the L-type calcium-channel blocker verapamil.

Conclusion Preconditioning with the ROCK inhibitor Y-27632 increased the engraftment of transplanted hiPSC-CM in a murine MI model, while reversibly impairing hiPSC-CM contractility and promoting adhesion.

Keywords Cardiac • Cell signalling • Cellular therapy • Induced pluripotent stem cells

1. Introduction

Stem- and progenitor-cell-based therapies are among the most promising strategies for promoting myocardial repair in patients with cardiac disease.[1,2] However, the effectiveness of these treatments is believed to be limited by the low proportion of cells that are retained and survive at the site of administration (i.e. the engraftment rate).[3] Many of the transplanted cells are lost to ischaemia, inflammation, and other cytotoxic outcomes of tissue injuries,[4] and therefore, attempts to increase the engraftment rate often focus on approaches aimed at improving cell survival, including genetic modifications[5]; treatment with prosurvival factors,[6] pharmacological agents,[7] or exosomes,[8,9] as well as hypoxic[10] or heat-shock preconditioning.[11] However, when murine embryonic stem cells were delivered to the uninjured myocardium of athymic nude rats, only approximately 40% of the administered cells remained at the delivery site for 3–5 h,[12] which suggests that a substantial proportion of

* Corresponding authors. Tel: +1 205 934 0228; fax: +1 205 934 9101, E-mail: wzhu@uab.edu (W.Z.); Tel: +1 205 934 8421; fax: +1 205 934 9101, E-mail: jayzhang@uab.edu (J.Z.)

the transplanted cells failed to adhere to the native tissues and were lost to the peripheral circulation. This observation may also explain why approaches towards restricting passive cell movement, such as the transplantation of engineered tissues rather than individual cells,[13,14] or creating a physical barrier that may prevent injected cells from leaking out through the needle track,[15] are often associated with higher rates of engraftment.

Cell adhesion and migration are implemented through cytoskeletal changes, many of which are regulated by Rho-associated, coiled-coil-containing protein kinases (ROCKs)[16]; ROCK1 is expressed in lung, liver, spleen, kidney and testis, while ROCK2 is primarily expressed in the heart and brain.[17] Both isoforms are inhibited by Y-27632, a cell-permeable small molecule that competes with ATP for access to the ROCK catalytic site[18,19] and is widely used to protect cultured stem/progenitor cells during their passaging.[20] Y-27632 also attenuates the contractile activity of smooth-muscle cells by reducing calcium sensitivity.[21] Here, we investigated whether the effect of Y-27632 preconditioning on cardiomyocyte (CM) adhesion and contraction can improve the engraftment rate of the injected cells in a murine model of myocardial infarction (MI). The transplanted CMs were differentiated from human-induced pluripotent stem cells (hiPSC), which have been extensively studied for use in regenerative therapies because they can be derived from reprogrammed somatic cells of any patient and then used to generate a theoretically unlimited number of cells of any lineage that can be re-administered to the same patient without provoking an immune response.[15]

2. Methods

2.1 hiPSC-derived CM differentiation and culturing conditions

The hiPSCs were reprogrammed from human cardiac fibroblasts as described previously,[22] transfected with a luciferase reporter gene,[23] and maintained on Matrigel Membrane Matrix (Thermo Fisher Scientific) in mTeSR^{TM} medium (Stem Cell Technologies) until 75% confluency and CM differentiation was performed by using a small molecule-based protocol, described previously.[24] Briefly, the cells were cultured in basal medium (RPMI 1640 medium supplemented with 2% B27 supplement minus insulin) with CHIR99021 (a GSK-3 inhibitor) for 24 h and in CHIR99021-free basal medium for 48 h; then, IWR-1 (a Wnt inhibitor) was added, and the cells were cultured for another 48 h before the medium was replaced with fresh basal medium, containing B27 supplement without insulin. Beating hiPSC-derived CM (hiPSC-CM) began to appear 9–12 days after differentiation was initiated. Y-27632 preconditioning consisted of a 12 h culture period in 10 μM Y-27632. Similarly, verapamil preconditioning consisted of a 12 h culture period in 1 μM of verapamil. Day 28 (4 weeks after initiation of cardiomyocyte differentiation) hiPSC-CMs were used for transplantation as we described before.[23] Before transplantation, the hiPSC-CMs were washed with phosphate-buffered saline (PBS), dissociated with 0.25% Trypsin (Cat# MT25-53CI, Fisher Scientific Inc.), centrifuged at 1000 rpm for 5 min, and resuspended in PBS.

2.2 MI and cell transplantation

All animal procedures were approved by the Institutional Animal Care and Use Committee (IACUC) of the University of Alabama at Birmingham and performed in accordance with the National Institutes of Health Guide for the Care and Use of Laboratory Animals (NIH publication No 85-23). MI was induced in NOD/SCID mice (2–4 months of age, body weight 20–25 g; The Jackson Laboratory, Stock Number 001303) as described previously.[23] Briefly, mice were anaesthetized with inhaled isoflurane (1.5–2%), intubated, and ventilated; then, a left thoracotomy was performed, and the left anterior descending coronary artery was ligated with an 8-0 non-absorbable suture. Immediately after MI, animals in the hiPSC-CM^{-RI} group were treated with hiPSC-CM that had been cultured under standard conditions, animals in the hiPSC-CM^{+RI} group were treated with hiPSC-CM that had been cultured with 10 μM of the ROCK inhibitor Y-27632 for 12 h, and animals in the PBS group were treated with an equivalent volume of PBS. Similarly, animals in the hiPSC-CM^{-VER} group were treated with hiPSC-CM that had been cultured under standard conditions, animals in the hiPSC-CM^{+VER} group were treated with hiPSC-CM that had been cultured with 1 μM of verapamil for 12 h. The treatments were administered via intramyocardial injection at three sites (3×10^5 cells/animal, 1×10^5 cells/site); one site was located in the infarcted region, and two were located in the region surrounding the infarct. The chest muscles and skin were closed, and the mice received intraperitoneal injections of buprenorphine (0.1 mg/kg) every 12 h for up to 3 days and intraperitoneal injections of carprofen (5 mg/kg) every 12 h for up to 1 day after surgery. After terminal studies at the indicated time points, animals were sacrificed under isoflurane inhalation followed by cervical dislocation.

2.3 Engraftment rate

Engraftment was determined both via *in vivo* bioluminescence imaging (BLI)[25] and by histological assessment of series of histological heart sections, stained for expression of the human variant of cardiac troponin T (hcTnT) and human nuclear antigen (HNA).[23] BLI was performed at the University of Alabama at Birmingham Small Animal Imaging Shared Facility with a Xenogen IVIS-100 system. Mice were anaesthetized with isoflurane and intraperitoneally injected with a luciferase substrate D-luciferin (375 mg/kg body weight); 10 min later, after luciferin reached mouse hearts via circulation and became converted to optically active oxyluciferin,[26] the number of engrafted cells was determined by comparing BLI signal intensity in the anterior left chest region to a standard curve generated from BLI measurements of known quantities (0.5×10^4, 1×10^4, 5×10^4, 1×10^5, 3×10^5, and 5×10^5) of luciferase-expressing hiPSC-CM.[25] For histological assessments, double-positive cells were counted in every 10th serial section of the whole heart, and the calculated total cell number in all analysed sections was multiplied by 10 to obtain the total number of engrafted hiPSC-CM per heart. The engraftment rate was then calculated by dividing the number of engrafted hiPSC-CM by the number of cells injected and expressed as a percentage.

2.4 Histological assessments

Histological assessments were performed with cultured cells and cryopreserved sections as described previously,[24] following IHC staining with the corresponding primary and secondary antibodies (Supplementary material online, *Table S1*). Tumour formation was assessed by histology as described before.[23] A thorough histopathological investigation did not reveal any myocardial nodule or mass. Besides, immunostaining of grafted cells was negative with commonly used tumour markers including carcinoembryonic antigen, α-fetoprotein, CA-125, and S-100 (data not shown).

2.5 Hypoxia

hiPSC-CMs were pretreated with 10 μM Y-27632 (hiPSC-CM^{+RI}), CN03 (hiPSC-CM^{+RA}), or 1 μM verapamil (hiPSC-CM^{+VER}) for 12 h.

Untreated cells in a separate group were used as a control (hiPSC-CM^{-RI}, or hiPSC-CM^{-VER}). After 12 h treatment, cells in all three groups were enzymatically detached (0.25% trypsin containing 2% chicken serum) and replated onto new chamber slides that were recoated with matrigel. The cells were then placed into an incubator which supplied 1% O_2, 5% CO_2, and 94% N_2. After 12 h, 24 h, and 48 h of incubation, the cells were washed and fixed with 4% paraformaldehyde for half an hour, followed by apoptosis analysis as described below.

2.6 Apoptosis analysis

Apoptosis level in the cells was analysed with an ApopTag Apoptosis Detection kit, as directed by the manufacturer's instructions (Cat# S7100, Chemicon International, Billerica, MA, USA). Briefly, samples (i.e. cultured cells or cryopreserved tissue sections) were fixed with 4% paraformaldehyde for 20 min, washed in PBS, incubated with 75 μL of equilibration buffer for 5 min at room temperature, incubated with 55 μL of TdT enzyme for 1 h at 37°C, washed with stop buffer for 10 min, rinsed 3 times with saline, incubated with anti-digoxigenin conjugate for 30 min at room temperature, rinsed with PBS, and imaged by a fluorescence microscope. Assessments of cultured cells were repeated twice and, at least eight sections from the infarcted region and the border zone of the infarcted region were evaluated for each heart.

2.7 Western blot

Cells were lysed with ice-cold Protein Extraction Reagent (Fisher Scientific) containing both protease-inhibitor (Sigma-Aldrich) and phosphatase-inhibitor (Sigma-Aldrich) cocktails; then, proteins were quantified with Coomassie Blue (Pierce), and SDS-PAGE/western blot analysis was performed by using Precast Protein Gels (Bio-Rad), Trans-Blot Turbo Mini PVDF Transfer Packs (Bio-Rad), and PVDF membrane staining with the corresponding antibodies (Supplementary material online, *Table S1*) as described previously.[23] Western blot signal was analysed by densitometry using an Image J software.

2.8 Enzyme-linked immunosorbent assay (ELISA)

ELISA assays were performed by using different Quantikine ELISA kits purchased from R&D Inc. (cat. # HSTCS0, DVC00/SVC00/PDVC00, DVE00/SVE00/PDVE00, DFA00B, and DTA00C/STA00C/PDTA00C). In brief, 10 μM Y-27632 or 1 μM verapamil were added into the hiPSC-CMs culture medium for 12 h, while untreated cells in separate groups were used as a control. The cell culture supernatants were collected prior to experiment and stored at -20°C before use. First, 50 μL of assay diluent, contained in the ELISA kit, were added to each well followed by 200 μL of standard, sample, or control and mixed well. The plates were incubated for 2 h at room temperature on a horizontal shaker. The plates were then washed four times with 400 μL washing buffer per well each time. The antibody conjugates were added to each well in 200 μL volume. The plate was then incubated at room temperature for 1 h. The plates were again washed four times with the washing buffer. The enzymatic colour reaction was carried out by adding 200 μL of substrate solution to each well and incubation of the plate at room temperature for 20 min. Lastly, 50 μL of stop solution were added to each well and the colour change of the solution in each well from blue to yellow was monitored visually. The plates were analysed by BioTek Synergy Hybrid Plate Reader at 450 nm, 540 nm and 570 nm visible wave lengths and the concentration of the proteins were calculated based on the background-normalized absorbance.

2.9 Cell attachment assay

Mouse HL-1 cardiac muscle cells (Millipore, Inc. #SCC065) were cultured in RPMI 1640 medium supplemented with 10% FBS until 95–100% confluent; then, the hiPSC-CMs (with or without 10 μM of Y-27632 preconditioning for 12 h) were treated with 0.25% trypsin for detachment, resuspended in RPMI 1640 medium, and incubated with non-specific IgG or neutralizing antibodies against N-Cadherin and Integrin at 37°C for 1 h. The hiPSC-CMs (200 000 cells per well) were then added to the surface of the HL-1 monolayer. Floating hiPSC-CMs were collected and counted 2–4 h later, and the attached hiPSC-CMs were quantified by subtracting the number of floating hiPSC-CMs from the total number of hiPSC-CMs added to the feeder layer, and expressed as a percentage. To confirm the histology data, the attached hiPSC-CMs were subjected to BLI assay. The BLI signal was quantified and the number of attached hiPSC-CMs was determined by comparing BLI signal intensity of each sample to the standard curve.[23] The number of attached cells was normalized to the total number of cells loaded and expressed as percentage.

2.10 Calcium recording and contractility

hiPSC-CM preconditioned with Y-27632 (10 μM), Rho kinase activator (RA) (100 nM), verapamil (1 μM), or no preconditioning (mock-treated) were incubated at 37°C for 30 min in Phenol Red-free DMEM containing 0.02% (*w/v*) Pluronic F127 and 5 μM Fluo-4 AM. Cells were then washed in a dye-free medium three times and rested for 30 min to allow for de-esterification of the dye. Cells were then placed in a microincubation system (Harvard Apparatus), maintained at a temperature of 37°C, and perfused with Tyrode's Solution containing (in mmol/L): 140 sodium chloride, 1 magnesium chloride, 10 HEPES, 5 potassium chloride, 10 glucose, and 1.8 calcium chloride, titrated to a pH of 7.4 with sodium hydroxide. An Olympus IX-81 confocal microscope coupled with a Fluoview FV1000 laser scan head was used to record spontaneous calcium transients by employing an XT line-scan. Recordings were taken for cells with continued ROCK inhibitor treatment (+RI), ROCK activator treatment (+RA), or no treatment (-RI) in the perfusion solution, and from cells at 12 h, 24 h, 48 h, and 72 h after withdrawal of RI and RA. Calcium transient recordings were also taken for cells with and without 1 μM verapamil. Calcium transient recordings were processed and analysed using MATLAB R2016A (The MathWorks, Inc., Natick, MA, USA). Spontaneous contraction recordings were taken using transmitted light function of the Olympus IX-81 microscope and captured using a PCO 1200 s high speed camera. Contraction measurements were made by using an Image J software.

2.11 Statistical analysis

Experiments and data analysis were performed by two researchers in a blinded fashion, and data are presented as mean ± SEM. Significance ($P < 0.05$) was determined via a Student's *t*-test for comparisons between two groups and via a two-way ANOVA for comparisons among three or more groups.

3. Results

3.1 ROCK inhibition improves the survival of transplanted hiPSC-CMs

MI was surgically induced in mice and then the animals were subjected to intramyocardial injection of either PBS, or hiPSC-CM cultured under standard conditions (hiPSC-CM^{-RI}), or hiPSC-CMs cultured in the

presence of 10 μM ROCK inhibitor Y-27632 for 12 h (hiPSC-CM^{+RI}). Because the iPSC-derived CMs were of human origin and carried a luciferase reporter gene, the engraftment rate was determined both in living animals via *in vivo* BLI[25] (*Figure 1A* and *B*) and in histological heart sections of sacrificed animals by identifying cells that express the hcTnT or HNA (*Figure 1C*). The results from both analyses indicated that Y-27632 preconditioning significantly increased the engraftment rate: luciferase activity was approximately six-fold higher on Days 3, 7, and 28 following treatment with hiPSC-CM^{+RI}, than after administration of hiPSC-CM^{-RI} (*Figure 1B*, Supplementary material online, *Figure S1A*), and hcTnT/HNA-expressing cells were approximately seven-fold more abundant in hearts from hiPSC-CM^{+RI}-treated animals, than in hearts from animals in the hiPSC-CM^{-RI}-treatment group (*Figure 1C*, Supplementary material online, *Figure S1B*). We determined the proportion of HNA-positive cells that did or did not co-express hcTnT (i.e. hiPSC-derived CMs or non-CMs, respectively) at Day 28 after cell transplantation. Our results suggested that in hiPS-CM^{+RI} and hiPSC-CM^{-RI} treated hearts, 92–96% of the engrafted hiPSC-derived cells were cardiomyocytes (*Figure 1C*, Supplementary material online, *Figure S1C*).

To explore the mechanism by which ROCK inhibition enhances the engraftment rate of transplanted hiPSC-CMs, we first analysed apoptosis and cell cycle activity in the grafts. Y-27632 preconditioning was found to promote an anti-apoptotic effect in grafted hiPSC-CMs, as indicated by a significantly lower number of TUNEL-positive cells in sections from hiPSC-CM^{+RI}-hearts than in those from the hearts of hiPSC-CM^{-RI}-treated animals on Day 2 (*Figure 1D*, Supplementary material online, *Figure S1D*). Apoptosis level was low on Day 7 in both cell-treatment groups, suggesting that cells undergo apoptosis mainly during the first few days after cell transplantation. The amounts of hcTnT-expressing cells that were also positive for the proliferation marker Ki67 (*Figure 1E*, Supplementary material online, *Figure S1E*) in both cell-treatment groups on Days 7 and 28 were similar, suggesting that Y-27632 preconditioning did not affect cell cycle in the transplanted cells.

3.2 ROCK inhibition reversibly inhibits the contractile activity of hiPSC-CMs

Next, we studied how ROCK inhibition increased the survival of transplanted hiPSC-CMs. Y-27632 preconditioning was associated with substantial changes in the morphology of the transplanted cells: hiPSC-CM^{+RI} were significantly larger than hiPSC-CM^{-RI}, with greater cytoskeletal organization and a more defined, rod-like shape 7 days after transplantation (*Figure 2A*, Supplementary material online, *Figure S2A* and *B*). Although cell morphologies equalized between hiPSC-CM^{-RI} and hiPSC-CM^{+RI} at Day 28, the cell area of hiPSC-CM^{-RI} remained significantly less than that in hiPSC-CM^{+RI}. It was reported that Y-27632 reduces coronary and cerebral artery vasospasm in large-animal models.[27,28] In addition, Y-27632 appears to impede the contractile activity of smooth-muscle cells by reducing calcium sensitivity.[21] Another ROCK inhibitor Fasudil has been linked to downregulation of cardiac troponin I (cTnI) expression in rats.[29,30] These reports prompted us to perform *in vitro* studies to explain the observed correlation between changes in cell contractility and cell morphology, i.e. the mechanism whereby Y-27632 inhibits contractile activity of transplanted hiPSC-CMs, resulting in their well-developed morphology and improved survival.

First, we examined cell morphology of cultured hiPSC-CMs 12 h after dissociation and replating (*Figure 2B*, Supplementary material online, *Figure S2C* and *D*). In line with the *in vivo* data, hiPSC-CM^{+RI} displayed a well-developed morphology and larger cell area as compared to hiPSC-CM^{-RI}. Interestingly, cells (hiPSC-CM^{+RA}) treated with Rho/Rac/Cdc42 Activator I (ROCK activator)[31,32] revealed a clearly smaller cell area and more round shape as compared to hiPSC-CM^{-RI} or hiPSC-CM^{+RI}. This observation was consistent with higher magnification bright field microscopy images of the cells obtained from the same field of view at different time points (1 h, 3 h, 5 h, and 12h) after cell replating, which suggested that comparing to –RI groups, the proportion of rod- or irregular-shaped (other than round-shape) cells was increased in +RI groups and decreased in +RA groups (*Figure 2C*, Supplementary material online, *Figure S2E*). Interestingly, at 72 h after withdrawal RI and RA, while no difference was found between –RI and +RI groups, the cell area was significantly smaller in +RA groups comparing to –RI or +RI groups (*Figure 2B*, Supplementary material online, *Figures S2D* and *S3*). Second, we analysed apoptosis levels in hiPSC-CMs under a hypoxia condition by a TUNEL staining assay. During 12 h, 24 h, and 48 h of culturing under hypoxia conditions, the number of TUNEL-positive cells, grown without Y-27632 preconditioning (hiPSC-CM^{-RI}), gradually increased and even more increased in ROCK activator-treated CMs (hiPSC-CM^{+RA}), while the number of apoptotic cells was significantly reduced in cells preconditioned with ROCK inhibitor (hiPSC-CM^{+RI}) (*Figure 2D*, Supplementary material online, *Figure S2F*).

We further investigated whether ROCK inhibition reduces the contractile activity of cultured hiPSC-CM that might promote the observed cell morphology change. Compared to hiPSC-CM^{-RI}, the contractile activity of hiPSC-CM^{+RI} was reduced by 32%, but increased by 42% in hiPSC-CMs^{+RA} (*Figure 3A*, Supplementary material online, *Figure S4A*). Furthermore, hiPSC-CMs^{+RI} displayed a 41% reduction in peak calcium transient fluorescence and an 11% reduction in calcium transient duration (calculated to 50% recovery), as compared to hiPSC-CM^{-RI} (*Figure 3B*, Supplementary material online, *Figure S4B*). On the contrary, hiPSC-CMs^{+RA} exhibited a 48% increase in peak calcium transient fluorescence and a 13% increase in calcium transient duration, relative to hiPSC-CM^{-RI} (*Figure 3B*, Supplementary material online, *Figure S4B*). Neither ROCK inhibitor (Y-27632) nor activator (Rho/Rac/Cdc42 Activator I) promoted any significant change in the recovery time (*Figure 3B*, Supplementary material online, *Figure S4B*). Interestingly, pretreatment with Y-27632 for 12 h significantly inhibited expression of cTnI and cTnT (*Figure 3C*, Supplementary material online, *Figure 5A*), two subunits of troponin (Tn) protein that regulates cardiomyocyte contraction. In contrast, the 3rd subunit of troponin cTnC was not dramatically affected by Y-27632 preconditioning (*Figure 3C*, Supplementary material online, *Figure S5A*). The phosphorylation of myosin light chain 2 (p-MLC2), a target of Rho Kinase, was also reduced by Y-27632 pretreatment of CMs (*Figure 3C*, Supplementary material online, *Figure S5A*). Interestingly, all cells completely recovered from these inhibitory effects 72 h after Y-27632 withdrawal (*Figure 3D*, Supplementary material online, *Figure S5B*).

3.3 Inhibition of contractile activity by verapamil enhances the survival of transplanted hiPSC-CMs

To verify if transient contractile inhibition contributes to Y-27632-mediated protection of transplanted hiPSC-CMs, we studied cell morphology, contractility, and apoptosis of hiPSC-CMs treated with a potent L-type calcium-channel (LTCC) blocker verapamil, which has been reported to arrest contractility of rat ventricular cardiomyocytes in culture.[33] After trypsinization hiPSC-CMs were replated and treated with different concentrations of verapamil (0.1 μM, 1 μM, and 10 μM) for 12 h.

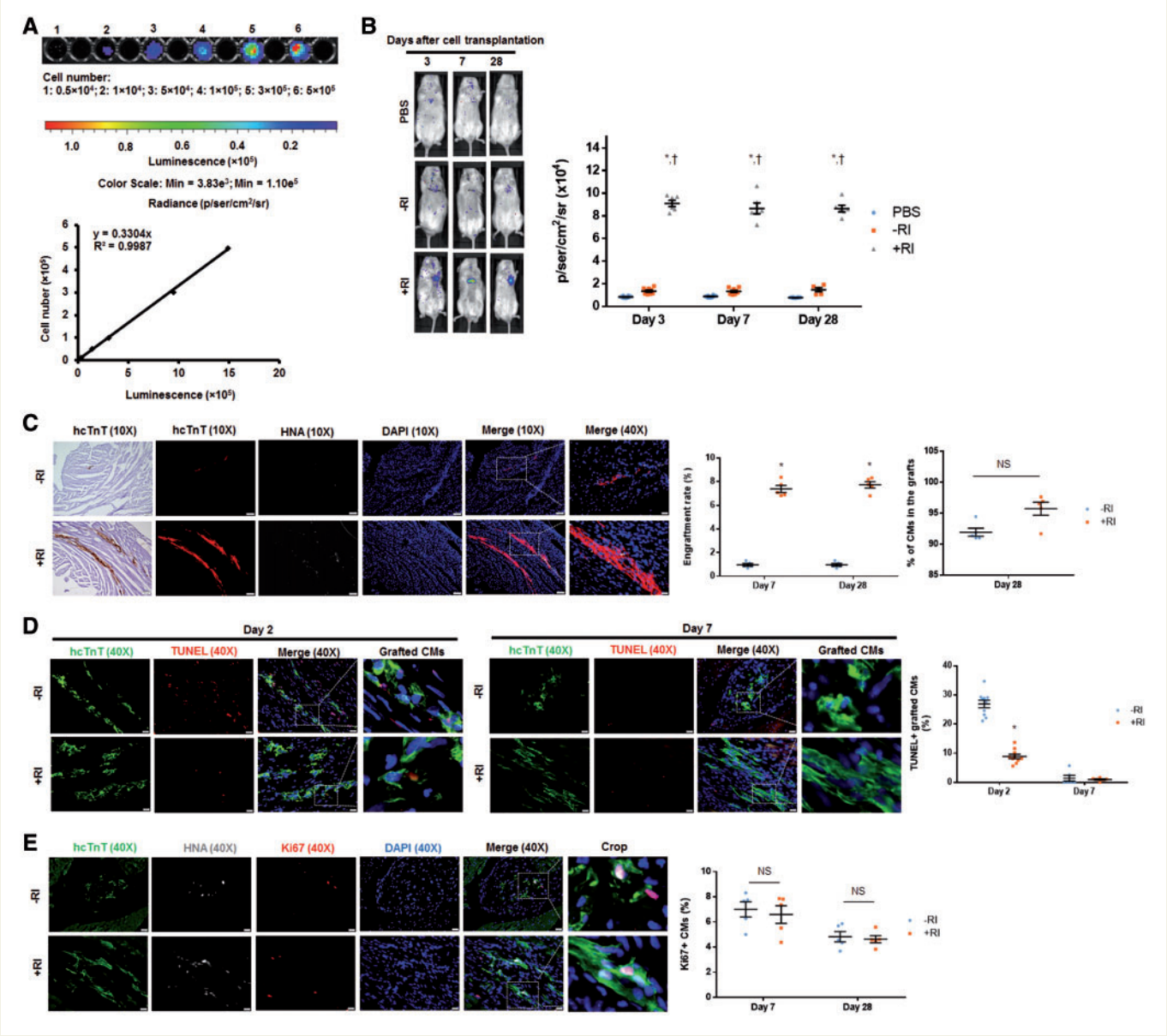

Figure 1 Y-27632 preconditioning improves engraftment rate of hiPSC-CMs transplanted into hearts of MI mice. Since transplanted cells carried a plasmid vector encoding a firefly luciferase reporter and were of human origin, the engraftment was evaluated via BLI and by identifying grafted cells that expressed the hcTnT and HNA. (*A*) A standard curve was generated from BLI measurements of various known hiPSC-CM cell numbers seeded on a plate. (*B*) Luciferin signal was higher in mice treated with hiPSC-CM^{+RI} than those treated with PBS or hiPSC-CM^{-RI} on Days 3, 7, and 28 after surgery. $n = 6$–9 mice per group. *$P < 0.05$ vs. PBS group; †$P < 0.05$ vs. hiPSC-CM^{-RI} group. (*C*) Heart sections from mice, sacrificed on Days 7 and 28 after surgery, were stained for hcTnT and HNA. Engraftment size was higher in mice receiving hiPSC-CM^{+RI} than those receiving hiPSC-CM^{-RI} on both Days 7 and 28 after surgery. Heart sections were stained with wheat germ agglutinin to define the cell border and with antibodies against HNA and hcTnT. The proportion of HNA-positive cells that also co-expressed hcTnT was determined and expressed as a percentage. (*C*) Images were obtained from animals on Day 28 after surgery. For 10X images: bar = 100 μm; for 40X images: bar = 20 μm. $n = 5$ mice per group; 32–40 sections per mice were evaluated. *$P < 0.05$ vs. hiPSC-CM^{-RI} group; unpaired Student's *t*-test was performed. (*D*–*E*) Cells undergoing apoptosis were identified by TUNEL staining. Cells with active cell cycle were identified by immunostaining for Ki67. The percentage of TUNEL+/hcTnT+ hiPSC-CMs (*D*) and Ki67+ hiPSC-CMs (*E*) was calculated. (*E*) Images were taken on Day 28 after surgery. (*D* and *E*) Bar = 20 μm. $n = 4$–6 mice per group; four sections per mice were evaluated. *$P < 0.05$ vs. hiPSC-CM^{-RI} group. One-way ANOVA analysis with Bonferroni correction was performed (*B*). Unpaired Student's *t*-test was performed (*C*–*E*). Data were presented as the mean ± SEM.

Cell morphology changes were detected via phalloidin staining. Our data suggest that verapamil promotes morphological development of hiPSC-CMs and increased cell area in a dose dependent manner (*Figure 4A*, Supplementary material online, *Figure S6A*). We then studied the effect of verapamil on contractility of hiPSC-CMs. Similar to Y-27632 preconditioning, treatment with verapamil (1 μM) for 12 h resulted in a 76% reduction in hiPSC-CM contractility (*Figure 4B*, Supplementary material online, *Figure S6B*), which is consistent with previous report that this

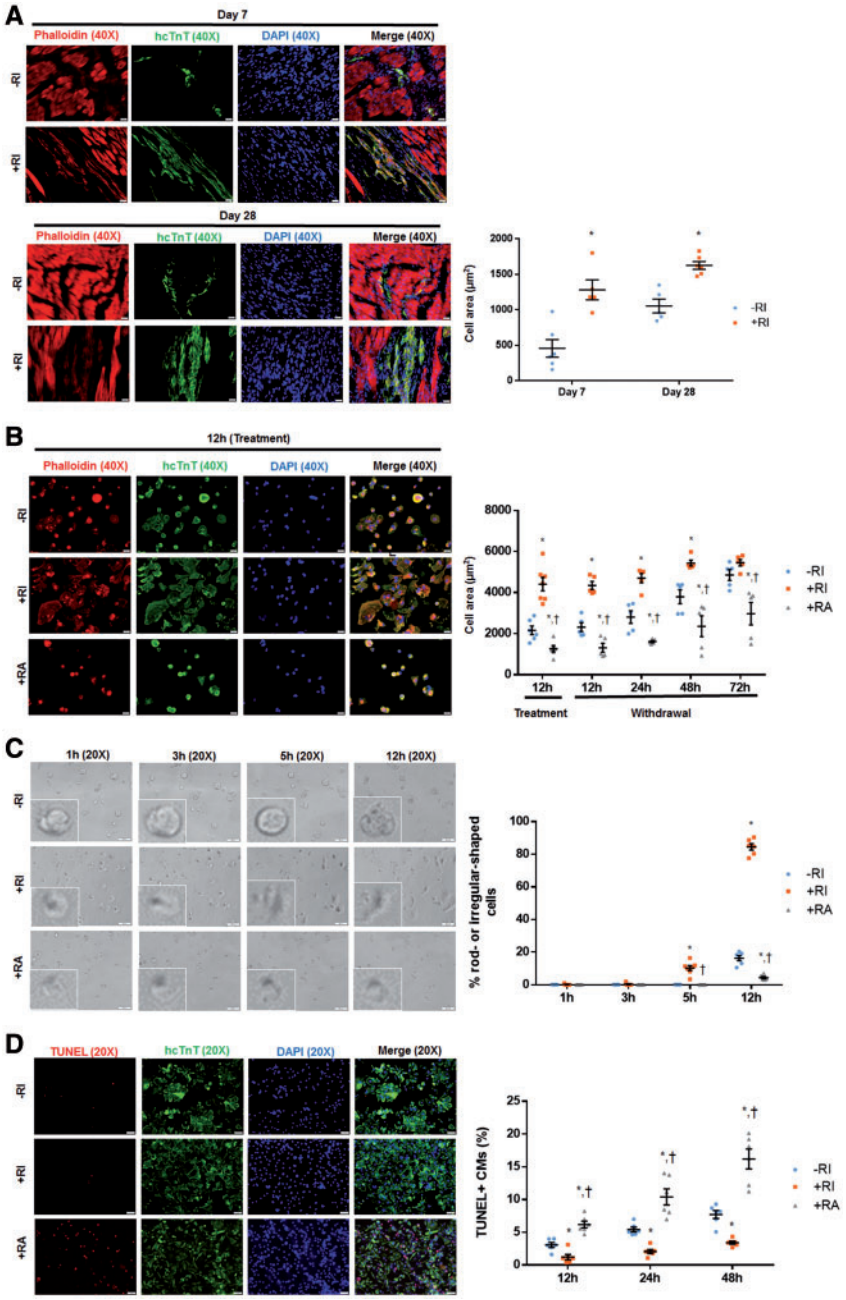

Figure 2 Y-27632 preconditioning changes morphology of hiPSC-CMs *in vivo* and *in vitro*, and increases their resistance to hypoxia-induced apoptosis. hiPSC-CMs were identified by immunostaining for hcTnT and cell morphology was revealed through phalloidin staining both *in vivo* and *in vitro*. (*A*) Seven days after cell transplantation, hiPSC-CM^{+RI} displayed a rod-shaped morphology, whereas hiPSC-CM^{-RI} exhibited an irregular shape. Sections were stained with wheat germ agglutinin to define the cell border. The cell area of hiPSC-CMs^{+RI} was significantly increased comparing to hiPSC-CMs^{-RI}. Twenty-eight days after cell transplantation, both hiPSC-CM^{+RI} and hiPSC-CM^{-RI} displayed a rod-shaped morphology. The cell area of hiPSC-CMs^{+RI} remained significantly higher comparing to hiPSC-CMs^{-RI}. Bar = 20 μm. $n = 5$ mice per group. *$P < 0.05$ vs. hiPSC-CM^{-RI}. (*B*) Twelve hours after replating and treatment (RI or RA), Y-27632-preconditioned CMs (+RI) exhibited a well-organized F-actin filaments and a more extended shape than non-preconditioned CMs (-RI) or ROCK activator (Rho/Rac/Cdc42 Activator I)- preconditioned cells (+RA) in culture. Consistent with *in vivo* data, the cell area of hiPSC-CM^{+RI} was significantly larger comparing to hiPSC-CM^{-RI} and hiPSC-CM+^{RA}. At 72 h after withdrawal of RI and RA, while no difference was found between –RI and +RI groups, cells in +RA groups remained significantly smaller than –RI and +RI groups. Bar = 20 μm. $n = 6$ replicates per group. *$P < 0.05$ vs. hiPSC-CM^{-RI}; †$P < 0.05$ vs. hiPSC-CM^{+RI}. (*C*) To track changes in cell morphology, a series of images for the same field of view were captured at different time points (1 h, 3 h, 5 h, and 12 h) after replating and treatment (RI or RA). While hiPSC-CMs^{+RI} started developing a rod-shape morphology at 5 h after seeding, hiPSC-CM^{-RI} or ROCK activator-preconditioned CMs (hiPSC-CM^{+RA}) remained round-shaped even at 12 h. The number of rod- or irregular-shaped (other than round-shape) cells was counted and presented as a percentage of total number of cells under the microscopic field. Bar = 50 μm. $n = 6$ replicates per group.

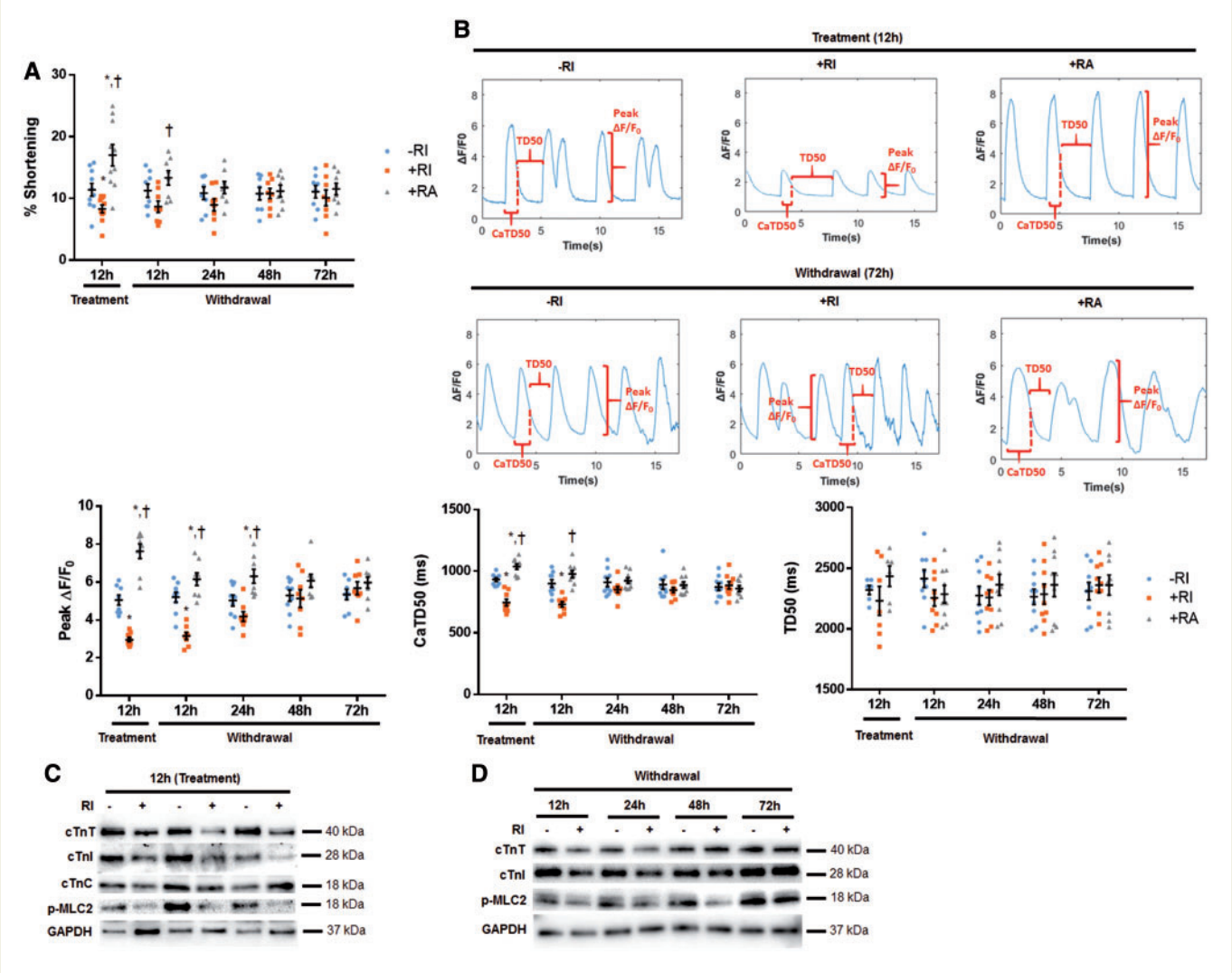

Figure 3 Y-27632 preconditioning reduces contractility of hiPSC-CMs and downregulates expression of cardiac troponin (cTn) subunits. hiPSC-CMs were enzymatically digested and replated on glass coverslip. hiPSC-CMs were subjected to a contractility and calcium transient assays 12 h after preconditioning with ROCK inhibitor (Y-27632, 10 μM), and at 12 h, 24 h, 48 h, and 72 h after Y-27632 withdrawal. For Western blot analysis, hiPSC-CMs were enzymatically detached and replated onto a six-well plate and whole cell lysates were prepared. The RI treatment resulted in reduced contractility (*A*) and calcium transients (*B*), as indicated by the decreased peak calcium transient fluorescence (peak $\Delta F/F_0$) and the calcium transient duration (calculated to 50% recovery, CaTD50). Conversely, the RA treatment resulted in an increase in peak calcium transient fluorescence and an increase in calcium transient duration. Neither Y-27632 nor ROCK activator resulted in any significant change in recovery time (TD50). The difference between the three groups was equalized at 48–72 h after withdrawal from RI or RA, suggesting these electrophysiological changes were transient. $n = 10$–11 cells per group. $^*P < 0.05$ vs. hiPSC-CM^{-RI}; $^\dagger P < 0.05$ vs. hiPSC-CM^{+RI}. (*C*) Western blot showing a reduced expression of cardiac troponin subunits (cTnT and cTnI), but not cTnC, and a decreased phosphorylation of MLC2 (a substrate of ROCK) in hiPSC-CM^{+RI}. (*D*) Western blot showing the Y-27632-induced inhibition of contractile regulatory proteins (troponins and phosphorylated MLC2) that was transient and recovered 72 h after the drug withdrawal. (*C* and *D*) $n = 5$–7 sample replicates per group. $^*P < 0.05$ vs. -RI. One-way ANOVA analysis with Bonferroni correction was performed (*A* and *B*). Data were presented as the mean ± SEM.

Figure 2 Continued

$^*P < 0.05$ vs. hiPSC-CM^{-RI}; $^\dagger P < 0.05$ vs. hiPSC-CM^{+RI}. (*D*) After dissociation and replating, hiPSC-CMs were treated with chemicals (RI or RA), and were cultured under hypoxia condition. TUNEL staining was performed to assess apoptosis of hiPSC-CMs^{+RI} under hypoxia condition at different time points (12 h, 24 h, and 48 h). ROCK inhibitor protected hiPSC-CMs from hypoxia-induced apoptosis, as indicated by a reduced level of apoptosis in hiPSC-CMs^{+RI} as compared to hiPSC-CM^{-RI} or hiPSC-CM^{+RA}. In addition, ROCK activator sensitized hiPSC-CMs to hypoxia-induced apoptosis. Bar = 50 μm. $n = 6$ replicates per group. $^*P < 0.05$ vs. hiPSC-CM^{-RI}; $^\dagger P < 0.05$ vs. hiPSC-CM^{+RI}. Unpaired Student's *t*-test was performed (*A*). One-way ANOVA analysis with Bonferroni correction was performed (*B*–*D*). Data were presented as the mean ± SEM.

dose of verapamil is sufficient to inhibit contraction of rat ventricular cardiomyocytes effectively.[34] Besides, verapamil treatment resulted in a 56% reduction in peak calcium transient fluorescence as well as a 26% reduction in calcium transient duration. This treatment also resulted in a 63% reduction in the recovery time (*Figure 4C*, Supplementary material online, *Figure S6C*). Based on the data presented with RI, it cannot be excluded that these effects with verapamil is transient. The impact of verapamil (1 μM) on apoptosis of hiPSC-CMs during 12 h, 24 h, and 48 h of hypoxia was also assessed by TUNEL staining. Our data revealed that verapamil inhibited hypoxia-induced apoptosis for all three time points (*Figure 4D*, Supplementary material online, *Figure S6D*).

We also assessed the survival and morphology of verapamil-preconditioned hiPSC-CMs (hiPSC-CM^{+VER}) *in vivo*. Interestingly, verapamil preconditioning (1 μM, 12 h) significantly improved the engraftment efficiency of transplanted hiPSC-CMs in mice with induced MI, as revealed by the increased luciferase signal in bioluminescence assay (*Figure 5A*, Supplementary material online, *Figure S7A*) and the increased number of hcTnT/HNA double positive cells upon histological staining (*Figure 5B*, Supplementary material online, *Figure S7B*) of tissue specimens at both Days 7 and 28 after cell administration. Verapamil-preconditioned CMs (hiPSC-CMs^{+VER}) exhibited an increased cell area and a rod-like shape on Day 7 (*Figure 5C*, Supplementary material online, *Figure S7C*), as well as a reduced apoptotic activity on Days 2 and 7 (*Figure 5D*, Supplementary material online, *Figure* S7D), compared with the control (hiPSC-CMs^{-VER}) cells. Although cell morphologies equalized between hiPSC-CM^{-VER} and hiPSC-CM^{+VER} at Day 28, the cell area of hiPSC-CM^{-VER} remained less than that in hiPSC-CM^{+VER}. Overall, the percentage of apoptotic hiPSC-CMs were low (~0.5%) in both groups (-VER vs. +VER), and there was no difference between these two groups (data not shown). These data suggested that transiently blocking contraction of transplanted hiPSC-CMs promotes their survival under hypoxic conditions.

3.4 Transient inhibition of contractile activity does not interfere with intrinsic pro-angiogenic activity of grafted hiPSC-CMs

Paracrine effects exerted on infarcted hearts by transplanted cells have been demonstrated to be essential for myocardial regeneration.[9,35] We, therefore, determined if transient contractile inhibition of transplanted hiPSC-CMs by Y-27632 or verapamil affects such a paracrine function. To this end, the infarct border zone vasculature was assessed by CD31 immunostaining. Notably, vessel density throughout border zones of all the MI hearts showed a similar decrease by Day 7, regardless of the cell treatment. In contrast, vascular density significantly increased in hearts implanted with hiPSC-CMs^{+RI} relative to hearts injected with non-preconditioned hiPSC-CMs^{-RI} by Day 28 (*Figure 6A*, Supplementary material online, *Figure S8A*). A similar increase was observed for hearts implanted with hiPSC-CM^{+VER} relative to hiPSC-CM^{-VER}-implanted hearts (*Figure 6B*, Supplementary material online, *Figure S8B*). Therefore, it is unlikely that Y-27632 or verapamil treatments interfere with the intrinsic paracrine effects of grafted hiPSC-CMs. To characterize the paracrine effects of transplanted hiPSC-CMs, various ELISA-based assays were employed for direct quantification of various cytokines in supernatants from Y-27632- or verapamil-treated cells *in vitro*.[36] In those assays, the release of cell adhesion (VCAM1), pro-angiogenic (VEGF, FGF), pro-migratory (G-CSF), and pro-apoptotic (TNF-α) factors was compared in all the experimental groups (-RI vs. +RI, and –VER vs. +VER). Neither Y-27632 nor verapamil treatment changed the release of any of the above cytokines, except that Y-27632 preconditioning increased the release of a cell adhesion molecule VCAM1 (*Figure 6C* and *D*), which indicated that ROCK inhibition could promote cell adhesion of transplanted hiPSC-CMs.

3.5 ROCK inhibition increases hiPSC-CM adhesion

Although the efforts in improving cardiac cell engraftment rate have often focused on increasing cell survival and viability after transplantation into the cytotoxic environment of the infarcted tissue, a substantial number of cells may be simply lost by being washed out from the administration (injection) site by the peripheral circulation.

We conducted a series of *in vitro* experiments to determine whether the augmented engraftment, associated with ROCK inhibition in the implanted hiPSC-CMs, might also occur through the increase in adhesion of the injected cells (improved cell retention), in addition to the improved cell survival. Our rationale for anticipating an increase in cell adhesion was based upon the following considerations: (i) ROCK is the key participant in the mechanisms that regulate cytoskeletal reorganization,[37] (ii) Y-27632 is known to upregulate Ras-related C3 botulinum toxin substrate 1 (RAC1), which promotes cadherin-mediated cell adhesion,[38] and (iii) Y-27632 preconditioning appeared to promote expression of N-cadherin, integrin ß1 (a molecule that regulates cytoskeleton organization[39]), and Connexin 43 (Cx43), as shown by enhanced fluorescent intensity of immunostaining in cultured cells (Supplementary material online, *Figure S9*) and in tissue sections (Supplementary material online, *Figure S10*). Western blot data confirmed the upregulation of these proteins during Y-27632 treatment (*Figure 7A*, Supplementary material online, *Figure S11A*), and a gradual normalization of these proteins to a level similar to control (-RI) after Y-27632 withdrawal (*Figure 7B*, Supplementary material online, *Figure S11B*).

To validate the importance of N-cadherin and integrins in mediating hiPSC-CMs adhesion to the recipient mouse hearts, an *in vitro* cell attachment experiment was performed using the HL-1 as feeder cells. HL-1 is a mouse cardiomyocyte cell line that can be passaged and it phenotypically mimics adult mammalian cardiomyocyte.[40] The hiPSC-CMs were cultured with or without 10 μM Y-27632 for 12 h, followed by incubation with non-specific antibodies or antibodies against either N-Cadherin or Integrin ß1 and then seeded onto a monolayer of HL-1 feeder cells (*Figure 7C*). Two and four hours later, both immunofluorescence staining with anti-hcTnT antibody (*Figure 7D*, Supplementary material online, *Figure S12A*) and BLI analysis (*Figure 7E*, Supplementary material online, *Figure S12B*) of adherent cells were performed. The results indicated that significantly more CMs were attached to the underlying cell layer when hiPSC-CMs^{+RI} were used (with Y-27632 preconditioning) than in the case of hiPSC-CMs^{-RI}, and this difference could be obliterated by culturing the hiPSC-CM^{+RI} with N-cadherin-neutralizing or integrin-neutralizing antibodies for 1 h before seeding.

4. Discussion

One of the major obstacles to maximizing the effectiveness of cell therapy is the low number of cells that are retained and survive at the site of administration.[15,41] In this regard, the most noteworthy finding from the experiments reported here is our observation that the engraftment rate of hiPSC-CM increased approximately seven-fold, when the cells were preconditioned with a ROCK inhibitor Y-27632 prior to injection into

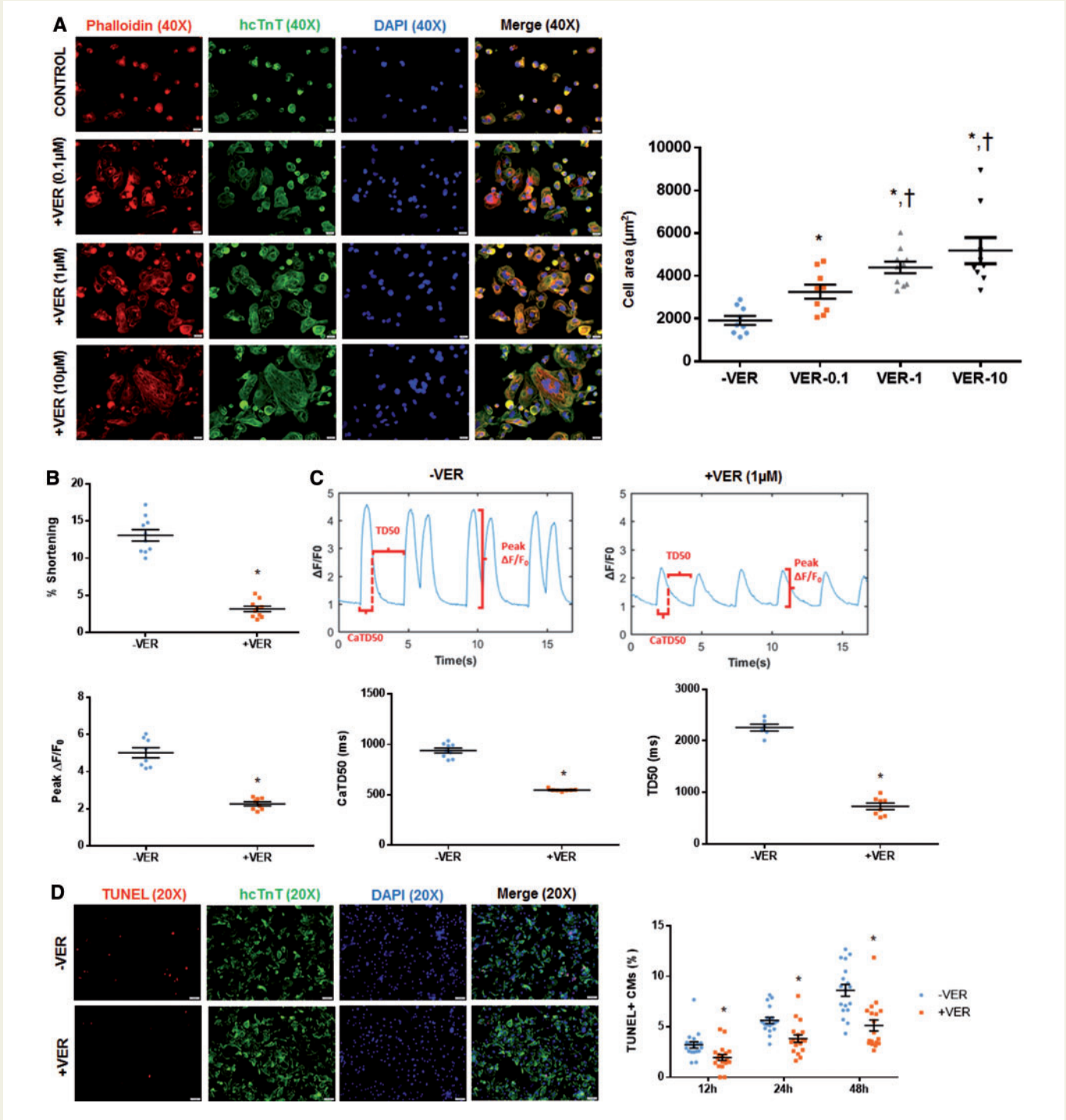

Figure 4 Verapamil preconditioning reduces contraction of hiPSC-CMs and enhances their resistance to hypoxia-induced apoptosis. Cultured hiPSC-CMs were treated with different concentration of verapamil (0.1 μM, 1 μM, or 10 μM), a potent LTCC inhibitor, for 12 h *in vitro*. hiPSC-CMs were identified by anti-hcTnT immunostaining, and cell morphology was analysed by phalloidin staining. For contractility studies, cells growing in glass coverslips were preconditioned for 12 h with verapamil (1 μM). (*A*) Similar to Y-27632 preconditioned cells, verapamil-preconditioned cells (hiPSC-CM^{+VER}) exhibited well-organized F-actin filaments and a more extended shape comparing to control cells (hiPSC-CM^{-VER}). The cell area of hiPSC-CMs^{+VER} significantly increased relative to hiPSC-CMs^{-VER} in a dose-dependent pattern. Bar = 20 μm. (*B*) hiPSC-CM^{+VER} displayed a reduced contractility relative to hiPSC-CMs^{-VER}. (*C*) Verapamil treatment also resulted in reduced peak calcium transient fluorescence (peak $\Delta F/F_0$) and duration (CaTD50), as well as reduced recovery time (TD50). (*D*) Impact of verapamil (1 μM) on apoptosis of hiPSC-CMs during 12 h, 24 h, and 48 h of hypoxia was assessed by TUNEL staining. Verapamil inhibited hypoxia-induced apoptosis at all three time points. Bar = 50 μm. (*A* and *D*) $n = 5$ replicates per group. *$P < 0.05$ vs. non-preconditioned cells; $P < 0.05$ vs. VER-0.1. (*B* and *C*) *$P < 0.05$ vs. hiPSC-CMs^{-VER}; $n = 10$–11 cells per group. One-way ANOVA analysis with Bonferroni correction was performed (*A*). Unpaired Student's *t*-test was performed (*B*–*D*). Data were presented as the mean ± SEM.

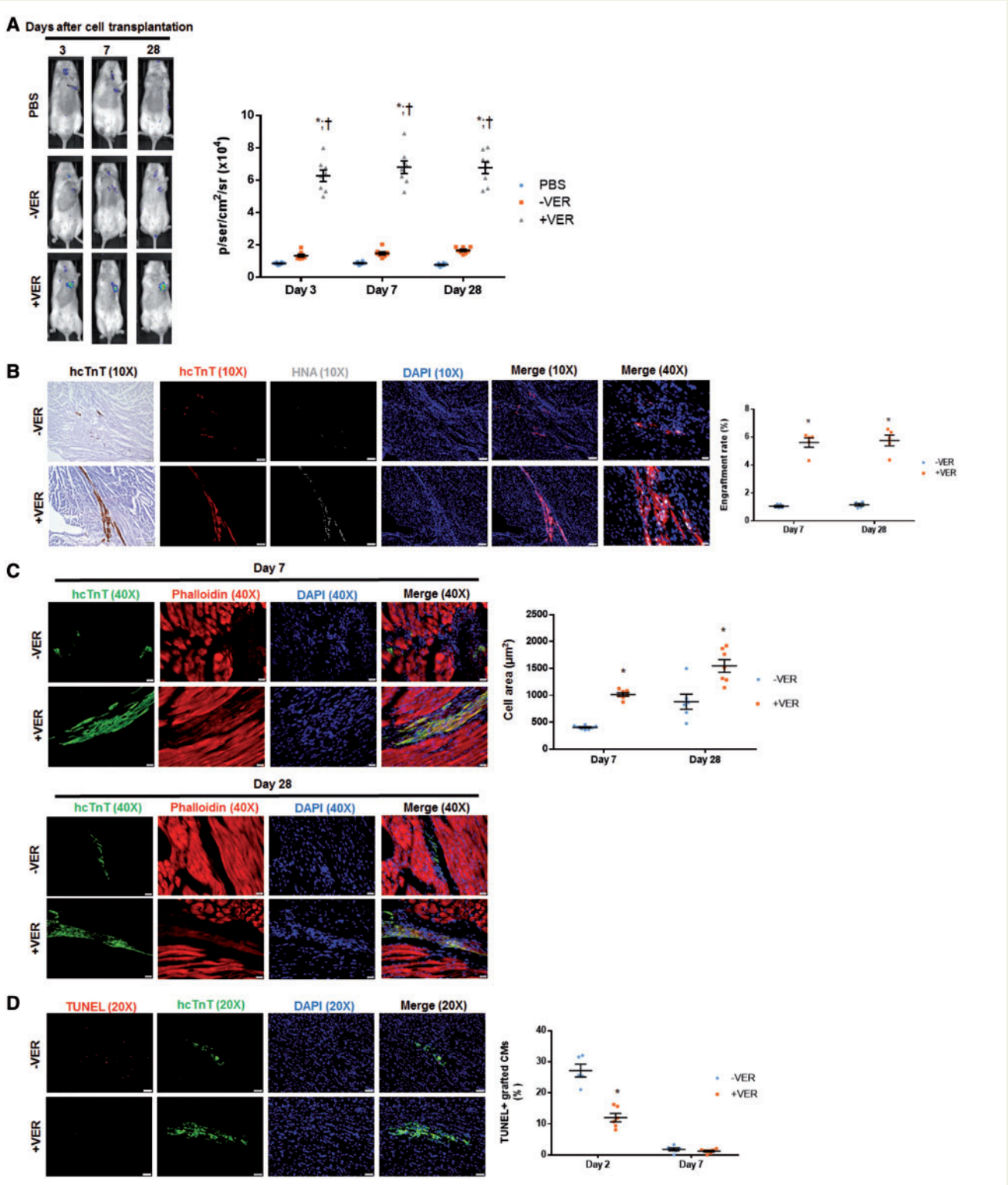

Figure 5 Preconditioning with verapamil improves transplantation of hiPSC-CMs in MI mice. (*A*) BLI was performed on Days 3, 7, and 28 past surgery to evaluate engraftment rate in live animals. $n = 8$ mice per group. $^{*}P < 0.05$ vs. PBS. $^{\dagger}P < 0.05$ vs. hiPSC-CMs^{-VER}. (*B*) Histological analysis was performed to analyse the presence of hcTnT and HNA in heart sections from mice that had been sacrificed on Days 7 and 28 after MI induction and hiPSC-CM injection. The engraftment rate was calculated by dividing the number of cells expressing both hcTnT and HNA by the total number of cells administered and expressed as a percentage. $n = 5$ mice per treatment group. For 10X images, bar = 100 μm; for 40X images, bar = 20 μm. (*C*) The morphology of grafted hiPSC-CMs was assessed by anti-hcTnT antibody and phalloidin tissue staining in the MI heart sections from mice that received either hiPSC-CMs^{+VER} or hiPSC-CMs^{-VER}. The cell area of hiPSC-CMs^{+VER} was significantly larger than that of hiPSC-CMs^{-VER} 7 days after transplantation, and this difference remained 28 days after transplantation. Bar = 20 μm. (*D*) Apoptotic cells were identified via TUNEL staining and the percentage of TUNEL-positive hiPSC-CMs was calculated. Bar = 20 μm. (*B*) Images were taken on Day 28 after cell transplantation, whereas images were obtained from animals sacrificed on Day 7 (*D*). (*C* and *D*) $n = 5$ mice per treatment group; with four sections per mice analysed; $^{*}P < 0.05$ vs. hiPSC-CM^{-VER} group. One-way ANOVA analysis with Bonferroni correction was performed (*A*). Unpaired Student's *t*-test was performed (*B*–*D*). Data were presented as the mean ± SEM.

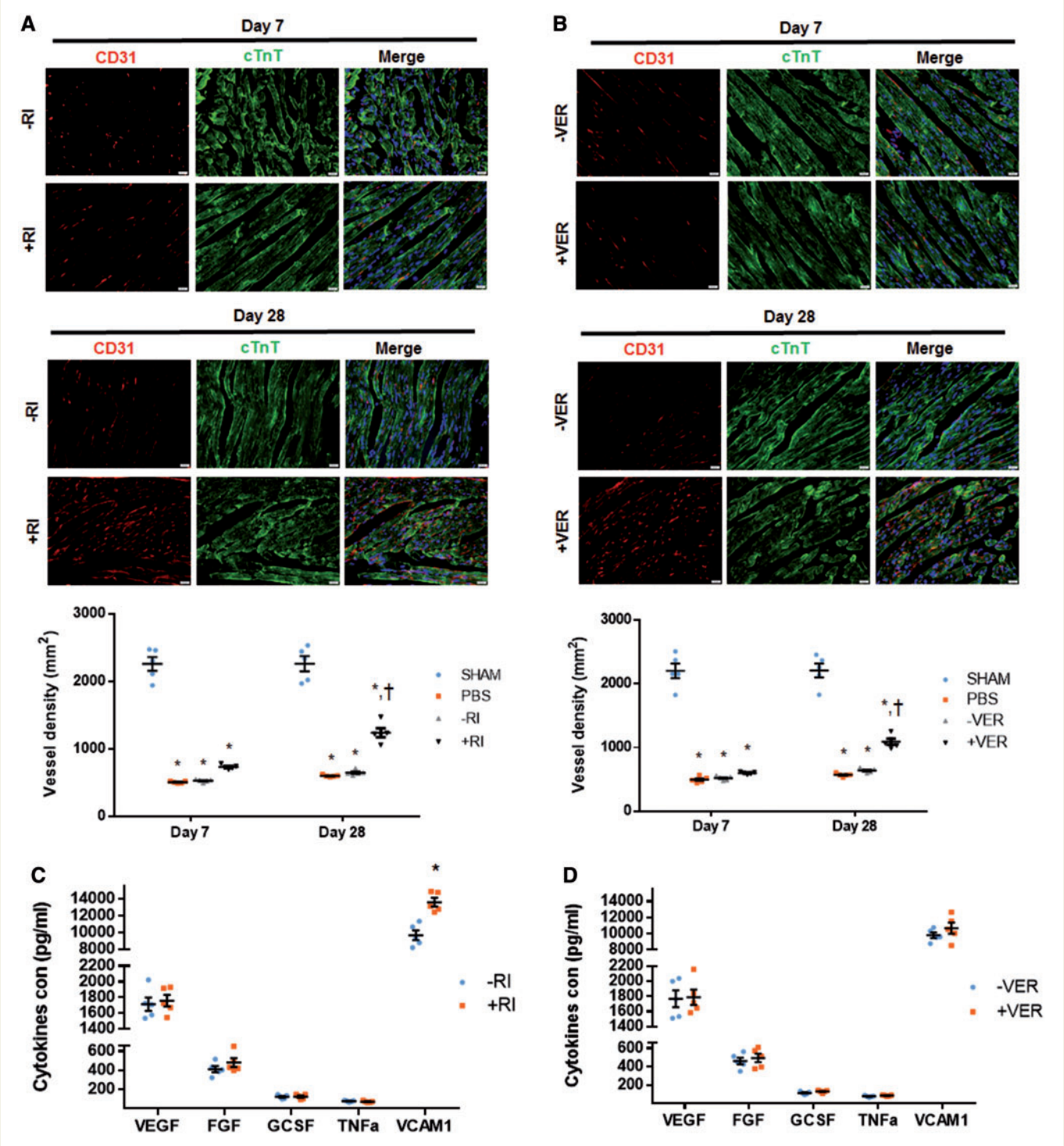

Figure 6 Transplantation of Y-27632 or verapamil-preconditioned hiPSC-CMs promotes angiogenesis in MI mice. (*A* and *B*) Tissue sections from the border-zone of MI hearts obtained from mice that received intramyocardial injection of (*A*) PBS-, hiPSC-CMs^{-RI}-, and hiPSC-CMs^{+RI}, or (*B*) PBS-, hiPSC-CM^{-VER}, and hiPSC-CM^{+VER} were immunofluorescently stained for the expression of CD31 and cTnT. Sections from the corresponding regions of the hearts from Sham mice were used as control. Vessel density was determined as the number of CD31-positive vascular structures per square millimetre. Bar = 20 μm. $n = 5$ mice per treatment group; four sections per mice were evaluated. *$P < 0.05$ vs. Sham mice; †$P < 0.05$ vs. MI mice. (*C* and *D*) Cell adhesion (VCAM1), pro-angiogenic (VEGF, FGF), pro-migratory (G-CSF), and pro-apoptotic (TNF-α) cytokines released from (*C*) hiPC-CM^{+RI} or (*D*) hiPC-CM^{+VER} *in vitro* were determined by ELISA. $n = 3$ replicates per group.* $P < 0.05$ vs. –RI group. One-way ANOVA analysis with Bonferroni correction was performed (*A* and *B*). Unpaired Student's *t*-test was performed (*C* and *D*). Data were presented as the mean ± SEM.

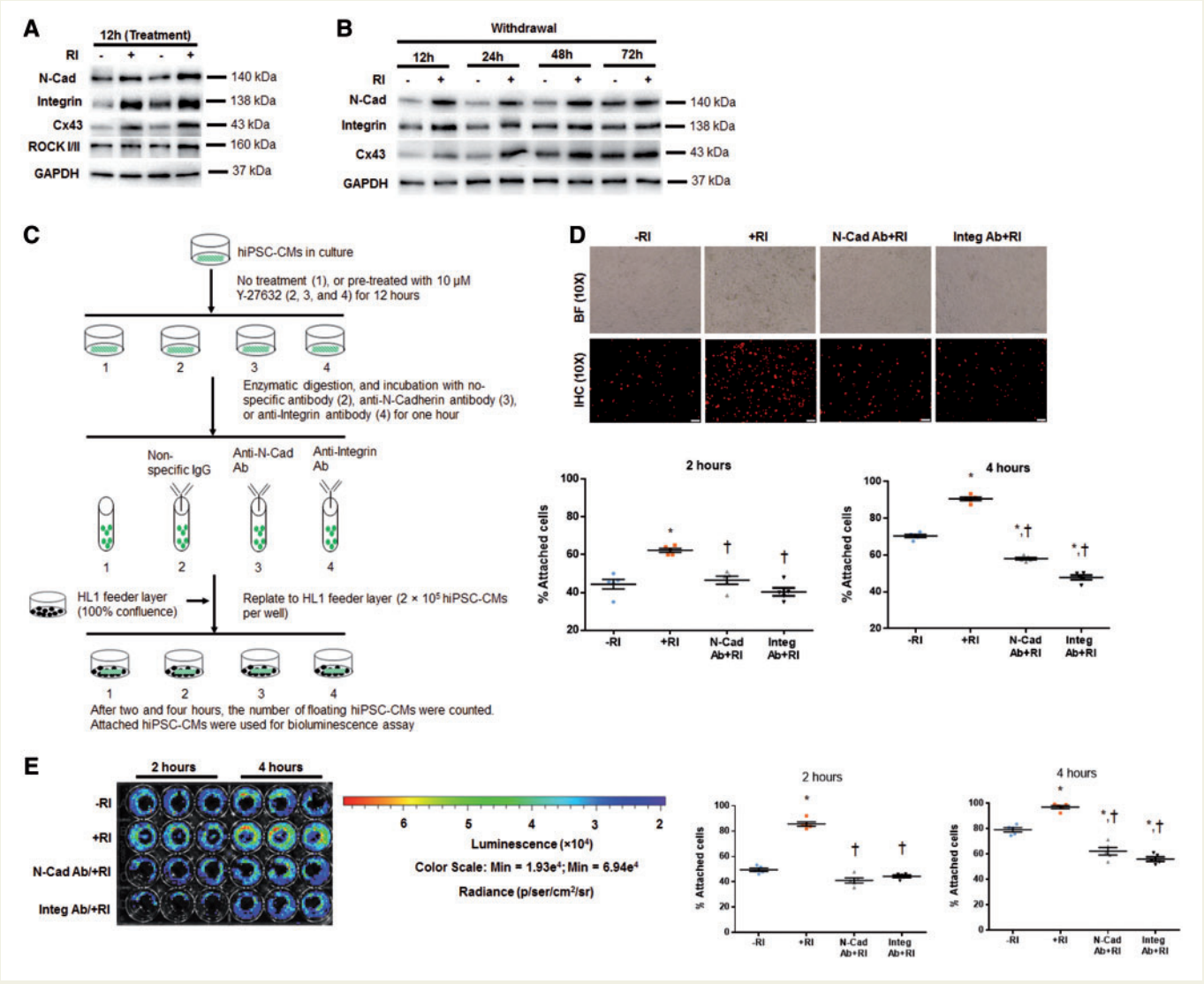

Figure 7 Y-27632 enhances adhesion of hiPSC-CMs via promoting formation of adherens junctions. (*A* and *B*) Western blot data confirmed the upregulated expression of N-Cadherin, Integrin ß1, and Cx43 in hiPSC-CMs^{+RI} at 12 h after cell passaging (relative to GAPDH) (*A*), and these differences were gradually normalized at 48–72 h after RI withdrawal (*B*). $n = 5$ replicates per group (*A* and *B*). Y-27632 preconditioning increases adhesion of hiPSC-CMs to the feeder layer, and this effect was partially abolished by pretreatment of CMs with anti-N-Cadherin or anti-Integrin ß1 antibodies. (*C*) Schematic representation of the adhesion experiment. (*D*) Immunofluorescence analysis of -RI and +RI hiPSC-CMs with and without their pretreatment with anti-N-Cadherin (N-Cad) and anti- and Integrin ß1 (Integ) antibodies. Attached hiPSC-CMs at 2 and 4 h after cell replating onto HL1 feeder layer were identified by immunostaining for hcTnT. The cell attachment rate was calculated by dividing the number of CMs attached to the feeder layer by the total number of CMs originally plated and expressed as a percentage. Bar = 100 μm. (*E*) Bioluminescence analysis of luciferase-expressing CMs treated as in *D*, and quantification of the attached cells (expressed as a percentage of total number of replated CMs), based on BLI signal quantification performed at 2 and 4 h time points; $n = 5$–7 replicates per group (*D* and *E*). $^{*}P < 0.05$ vs. hiPSC-CM^{-RI}; $^{\dagger}P < 0.05$ vs. hiPSC-CM^{+RI}. One-way ANOVA analysis with Bonferroni correction was performed (*D* and *E*). Data were presented as the mean ± SEM.

the infarcted hearts of mice. We also showed that the increase in the cell engraftment rate was accompanied by a reduction in the number of apoptotic hiPSC-CMs and unchanged proliferative activity. Y-27632 preconditioning also reduced the contractile activity of cultured hiPSC-CM. The latter could (at least in theory) improve the survival rate of transplanted hiPSC-CM by reducing their demand for ATP and other nutrients, which are relatively scarce in the infarcted region of the myocardium. However, the effect of Y-27632 on hiPSC-CM contraction efficiency was reversible and, consequently, did not affect the paracrine capabilities of transplanted hiPSC-CMs. Y-27632 preconditioning was also found to increase adhesion of the cultured hiPSC-CMs to the underlying layer of HL-1 feeder cells. Thus, we postulate that ROCK inhibition improves engraftment by transiently reducing CM contractility, enhancing survival of the transplanted cells, and increasing their adhesion to the native tissues at the site of administration, which subsequently reduces the number of cells that are lost to the peripheral circulation. Additional studies are needed to determine mechanisms by which Y-27632 treatment enhances engraftment.

The improved adhesion properties observed for the Y-27632-preconditioned hiPSC-CM were accompanied by an upregulated expression of junction proteins N-cadherin and integrins, which have been implicated in cell adhesion, migration, and growth.[42–45] Cadherin is also one of the three primary components of cardiac intercalated discs, structures unique to cardiac muscle cells. Studies in mice suggest that N-cadherin contributes to gap-junction formation, since an induced, cardiac-specific deletion of N-cadherin gene was found to be associated with lower levels of connexin expression, a decline in CM conduction velocity, and a spontaneous ventricular tachycardia.[46,47] In consistent with these, we also observed an increased connexin-43 (Cx43) expression in hiPSC-CM^{+RI} than hiPSC-CM^{-RI} *in vitro* (*Figure 7A*, Supplementary material online, *Figures S9* and *S11A*) and *in vivo* (Supplementary material online, *Figure S10A* and *B*). Thus, it is possible that Y-27632 preconditioning may enhance the coupling between grafted hiPSC-CMs with host myocardium after their recovery from a transient contractile inhibition via promoting gap junction formation.

Y-27632 preconditioning was also associated with a striking change in hiPSC-CM phenotype. Seven days after transplantation, preconditioned cells were noticeably larger and exhibited more myocyte-like appearance (a more defined rod-like shape and cytoskeletal organization) than cells cultured under standard conditions. In cultured cells similar morphological changes were recapitulated by CM treatment with either Y-27632 or an LTCC-blocker verapamil. Data on cell area changes after 12 h, compared with 24 h, 48 h, and 72 h shows that the effect of Y-27632 is transient. The fact that control cells (-RI) increase their cell area over time to match +RI cells after 72 h suggests that the initial effect may be via faster and more efficient adhesion of +RI cells to the plate or feeder cells compared to -RI cells, rather than an actual cell size change after Y-27632 treatment. Y-27632 significantly reduced the expression of cTnT and cTnI, which regulate CM contraction by forming a complex with cTnC (a troponin subunit which binds to intracellular Ca^{2+}). Collectively, the above observations suggest that reduction in the Ca^{2+}-induced contractile activity alone, rather than the more diverse changes associated with ROCK inhibition, may promote a more myocyte-like phenotype in transplanted and cultured hiPSC-CM. Calcium channel blockers are commonly used for treating patients with heart failure.[48] ROCK inhibitors are also being tested for treating patients with coronary heart diseases and heart failure.[49,50] When patients receiving hiPSC-CMs as a therapy are also receiving ROCK inhibitor or calcium channel blockers, a caution should be made that the systemic levels of these medications may inhibit the contraction of implanted hiPSC-CMs.

There are some limitations in our study: (i) a deeper analysis of sarcomere organization is warranted to further understanding how rock inhibitor preconditioning increases cell area and induces cardiomyocyte morphology and cytoskeletal organization, while decreases cTnT and cTnI expression as well as contractility. (ii) The contractility assays rely on fractional shortening which is semi-quantitative since cell shape and mechanical properties may be different. (iii) The contractility assays were performed on singularized cells which does not account for differences in gap junction function. Electrophysiological analysis is warranted given that verapamil also enhances engraftment and changes calcium handling.

In conclusion, the data presented here suggest that intramyocardial injection of hiPSC-CMs, preconditioned with a ROCK inhibitor Y-27632 prior to administration, significantly improves the cell engraftment rate. This improvement is likely to occur not only due to an increased cell survival, but also through an augmented cell adhesion properties promoted by upregulation of junctional proteins, such as integrins and N-cadherin. In addition, Y-27632 preconditioning reversibly impaired the contractile function of hiPSC-CMs, downregulated cTnI and cTnT expression, and led to striking morphological changes in CMs that could be recapitulated *in vitro* by a calcium-channel blocker verapamil. An attenuated contraction could potentially lower CM energy consumption, thereby increasing survival of transplanted hiPSC-CMs in ischaemic hearts. It is yet to be determined whether the engraftment rate could also be improved by genetic overexpression of junctional proteins and/or through the mechanism, whereby Y-27632 regulates the expression of cardiac troponins. Importantly, our results also suggest that various engineering approaches aimed at restricting the loss of transplanted cells from the implantation (administration) site due to their passive movement, such as methods for increasing a transplanted cell adhesion, could potentially improve cardiac cell engraftment.

Supplementary material

Supplementary material is available at *Cardiovascular Research* online.

Acknowledgements

We thank Joseph C. Wu (Stanford University) for kindly providing the Fluc-GFP construct, Yanwen Liu and Xi Lou for excellent technical assistance, and W. Kevin Cukier-Meisner for his editorial assistance.

Conflict of interest: none declared.

Funding

This study was supported by the National Institutes of Health (RO1 grants HL95077, HL114120, HL131017, HL138023, UO1 HL134764 to J.Z. and HL121206A1 to L.Z.), American Heart Association Scientist Development Grant (16SDG30410018 to W.Z.), and China Scholarship Council (to M.Z. and C.F.).

References

1. Zimmermann WH. Remuscularization of the failing heart. *J Physiol (Lond)* 2017;**595**:3685–3690.
2. Zimmermann WH. Translating myocardial remuscularization. *Circ Res* 2017;**120**:278–281.
3. Yanamandala M, Zhu W, Garry DJ, Kamp TJ, Hare JM, Jun HW, Yoon YS, Bursac N, Prabhu SD, Dorn GW 2nd, Bolli R, Kitsis RN, Zhang J. Overcoming the roadblocks to cardiac cell therapy using tissue engineering. *J Am Coll Cardiol* 2017;**70**:766–775.
4. Zhang M, Methot D, Poppa V, Fujio Y, Walsh K, Murry CE. Cardiomyocyte grafting for cardiac repair: graft cell death and anti-death strategies. *J Mol Cell Cardiol* 2001;**33**:907–921.
5. Mangi AA, Noiseux N, Kong D, He H, Rezvani M, Ingwall JS, Dzau VJ. Mesenchymal stem cells modified with Akt prevent remodeling and restore performance of infarcted hearts. *Nat Med* 2003;**9**:1195–1201.
6. Laflamme MA, Chen KY, Naumova AV, Muskheli V, Fugate JA, Dupras SK, Reinecke H, Xu C, Hassanipour M, Police S, O'Sullivan C, Collins L, Chen Y, Minami E, Gill EA, Ueno S, Yuan C, Gold J, Murry CE. Cardiomyocytes derived from human embryonic stem cells in pro-survival factors enhance function of infarcted rat hearts. *Nat Biotechnol* 2007;**25**:1015–1024.
7. Niagara MI, Haider H, Jiang S, Ashraf M. Pharmacologically preconditioned skeletal myoblasts are resistant to oxidative stress and promote angiomyogenesis via release of paracrine factors in the infarcted heart. *Circ Res* 2007;**100**:545–555.
8. Sahoo S, Klychko E, Thorne T, Misener S, Schultz KM, Millay M, Ito A, Liu T, Kamide C, Agrawal H, Perlman H, Qin G, Kishore R, Losordo DW. Exosomes from human CD34(+) stem cells mediate their proangiogenic paracrine activity. *Circ Res* 2011;**109**:724–728.
9. Khan M, Nickoloff E, Abramova T, Johnson J, Verma SK, Krishnamurthy P, Mackie AR, Vaughan E, Garikipati VN, Benedict C, Ramirez V, Lambers E, Ito A, Gao E, Misener S, Luongo T, Elrod J, Qin G, Houser SR, Koch WJ, Kishore R. Embryonic stem cell-derived exosomes promote endogenous repair mechanisms and enhance cardiac function following myocardial infarction. *Circ Res* 2015;**117**:52–64.

10. Hu X, Yu SP, Fraser JL, Lu Z, Ogle ME, Wang JA, Wei L. Transplantation of hypoxia-preconditioned mesenchymal stem cells improves infarcted heart function via enhanced survival of implanted cells and angiogenesis. *J Thorac Cardiovasc Surg* 2008;**135**:799–808.
11. Feng Y, Huang W, Meng W, Jegga AG, Wang Y, Cai W, Kim HW, Pasha Z, Wen Z, Rao F, Modi RM, Yu X, Ashraf M. Heat shock improves Sca-1^{+} stem cell survival and directs ischemic cardiomyocytes toward a prosurvival phenotype via exosomal transfer: a critical role for HSF1/miR-34a/HSP70 pathway. *Stem Cells* 2014;**32**:462–472.
12. Qiao H, Surti S, Choi SR, Raju K, Zhang H, Ponde DE, Kung HF, Karp J, Zhou R. Death and proliferation time course of stem cells transplanted in the myocardium. *Mol Imaging Biol* 2009;**11**:408–414.
13. Ye L, Basu J, Zhang J. Fabrication of a myocardial patch with cells differentiated from human-induced pluripotent stem cells. *Methods Mol Biol* 2015;**1299**:103–114.
14. Riegler J, Tiburcy M, Ebert A, Tzatzalos E, Raaz U, Abilez OJ, Shen Q, Kooreman NG, Neofytou E, Chen VC, Wang M, Meyer T, Tsao PS, Connolly AJ, Couture LA, Gold JD, Zimmermann WH, Wu JC. Human engineered heart muscles engraft and survive long term in a rodent myocardial infarction model. *Circ Res* 2015;**117**:720–730.
15. Ye L, Chang YH, Xiong Q, Zhang P, Zhang L, Somasundaram P, Lepley M, Swingen C, Su L, Wendel JS, Guo J, Jang A, Rosenbush D, Greder L, Dutton JR, Zhang J, Kamp TJ, Kaufman DS, Ge Y, Zhang J. Cardiac repair in a porcine model of acute myocardial infarction with human induced pluripotent stem cell-derived cardiovascular cells. *Cell Stem Cell* 2014;**15**:750–761.
16. Shi J, Wei L. Rho kinases in cardiovascular physiology and pathophysiology: the effect of fasudil. *J Cardiovasc Pharmacol* 2013;**62**:341–354.
17. Dong M, Yan BP, Liao JK, Lam YY, Yip GW, Yu CM. Rho-kinase inhibition: a novel therapeutic target for the treatment of cardiovascular diseases. *Drug Discov Today* 2010;**15**:622–629.
18. Ishizaki T, Uehata M, Tamechika I, Keel J, Nonomura K, Maekawa M, Narumiya S. Pharmacological properties of Y-27632, a specific inhibitor of rho-associated kinases. *Mol Pharmacol* 2000;**57**:976–983.
19. Davies SP, Reddy H, Caivano M, Cohen P. Specificity and mechanism of action of some commonly used protein kinase inhibitors. *Biochem J* 2000;**351**:95–105.
20. Watanabe K, Ueno M, Kamiya D, Nishiyama A, Matsumura M, Wataya T, Takahashi JB, Nishikawa S, Nishikawa S, Muguruma K, Sasai Y. A ROCK inhibitor permits survival of dissociated human embryonic stem cells. *Nat Biotechnol* 2007;**25**:681–686.
21. Fu X, Gong MC, Jia T, Somlyo AV, Somlyo AP. The effects of the Rho-kinase inhibitor Y-27632 on arachidonic acid-, GTPγS-, and phorbol ester-induced Ca^{2+}-sensitization of smooth muscle. *FEBS Lett* 1998;**440**:183–187.
22. Zhang L, Guo J, Zhang P, Xiong Q, Wu SC, Xia L, Roy SS, Tolar J, O'Connell TD, Kyba M, Liao K, Zhang J. Derivation and high engraftment of patient-specific cardiomyocyte sheet using induced pluripotent stem cells generated from adult cardiac fibroblast. *Circ Heart Fail* 2015;**8**:156–166.
23. Zhu W, Zhao M, Mattapally S, Chen S, Zhang J. CCND2 overexpression enhances the regenerative potency of human induced pluripotent stem cell-derived cardiomyocytes: remuscularization of injured ventricle. *Circ Res* 2018;**122**:88–96.
24. Gao L, Kupfer ME, Jung JP, Yang L, Zhang P, Da Sie Y, Tran Q, Ajeti V, Freeman BT, Fast VG, Campagnola PJ, Ogle BM, Zhang J. Myocardial tissue engineering with cells derived from human-induced pluripotent stem cells and a native-like, high-resolution, 3-dimensionally printed scaffold. *Circ Res* 2017;**120**:1318–1325.
25. Ong SG, Huber BC, Lee WH, Kodo K, Ebert AD, Ma Y, Nguyen PK, Diecke S, Chen WY, Wu JC. Microfluidic single-cell analysis of transplanted human induced pluripotent stem cell-derived cardiomyocytes after acute myocardial infarction. *Circulation* 2015;**132**:762–771.
26. Sun N, Lee A, Wu JC. Long term non-invasive imaging of embryonic stem cells using reporter genes. *Nat Protoc* 2009;**4**:1192–1201.
27. Sato M, Tani E, Fujikawa H, Kaibuchi K. Involvement of Rho-kinase-mediated phosphorylation of myosin light chain in enhancement of cerebral vasospasm. *Circ Res* 2000;**87**:195–200.
28. Shimokawa H, Seto M, Katsumata N, Amano M, Kozai T, Yamawaki T, Kuwata K, Kandabashi T, Egashira K, Ikegaki I, Asano T, Kaibuchi K, Takeshita A. Rho-kinase-mediated pathway induces enhanced myosin light chain phosphorylations in a swine model of coronary artery spasm. *Cardiovasc Res* 1999;**43**:1029–1039.
29. Mera C, Godoy I, Ramirez R, Moya J, Ocaranza MP, Jalil JE. Mechanisms of favorable effects of Rho kinase inhibition on myocardial remodeling and systolic function after experimental myocardial infarction in the rat. *Ther Adv Cardiovasc Dis* 2016;**10**:4–20.
30. Robertson SP, Johnson JD, Potter JD. The time-course of Ca2+ exchange with calmodulin, troponin, parvalbumin, and myosin in response to transient increases in Ca2+. *Biophys J* 1981;**34**:559–569.
31. Takito J, Otsuka H, Yanagisawa N, Arai H, Shiga M, Inoue M, Nonaka N, Nakamura M. Regulation of osteoclast multinucleation by the actin cytoskeleton signaling network. *J Cell Physiol* 2015;**230**:395–405.
32. Kuang SQ, Kwartler CS, Byanova KL, Pham J, Gong L, Prakash SK, Huang J, Kamm KE, Stull JT, Sweeney HL, Milewicz DM. Rare, nonsynonymous variant in the smooth muscle-specific isoform of myosin heavy chain, MYH11, R247C, alters force generation in the aorta and phenotype of smooth muscle cells. *Circ Res* 2012;**110**:1411–1422.
33. Bassani JW, Qi M, Samarel AM, Bers DM. Contractile arrest increases sarcoplasmic reticulum calcium uptake and SERCA2 gene expression in cultured neonatal rat heart cells. *Circ Res* 1994;**74**:991–997.
34. Bell D, McDermott BJ. Inhibition by verapamil and diltiazem of agonist-stimulated contractile responses in mammalian ventricular cardiomyocytes. *J Mol Cell Cardiol* 1995;**27**:1977–1987.
35. Gnecchi M, He H, Liang OD, Melo LG, Morello F, Mu H, Noiseux N, Zhang L, Pratt RE, Ingwall JS, Dzau VJ. Paracrine action accounts for marked protection of ischemic heart by Akt-modified mesenchymal stem cells. *Nat Med* 2005;**11**:367–368.
36. Tachibana A, Santoso MR, Mahmoudi M, Shukla P, Wang L, Bennett M, Goldstone AB, Wang M, Fukushi M, Ebert AD, Woo YJ, Rulifson E, Yang PC. Paracrine effects of the pluripotent stem cell-derived cardiac myocytes salvage the injured myocardium. *Circ Res* 2017;**121**:e22–e36.
37. Loirand G, Sauzeau V, Pacaud P. Small G proteins in the cardiovascular system: physiological and pathological aspects. *Physiol Rev* 2013;**93**:1659–1720.
38. Noritake J, Watanabe T, Sato K, Wang S, Kaibuchi K. IQGAP1: a key regulator of adhesion and migration. *J Cell Sci* 2005;**118**:2085–2092.
39. Defilippi P, Venturino M, Gulino D, Duperray A, Boquet P, Fiorentini C, Volpe G, Palmieri M, Silengo L, Tarone G. Dissection of pathways implicated in integrin-mediated actin cytoskeleton assembly. Involvement of protein kinase C, Rho GTPase, and tyrosine phosphorylation. *J Biol Chem* 1997;**272**:21726–21734.
40. Claycomb WC, Lanson NA Jr, Stallworth BS, Egeland DB, Delcarpio JB, Bahinski A, Izzo NJ Jr. HL-1 cells: a cardiac muscle cell line that contracts and retains phenotypic characteristics of the adult cardiomyocyte. *Proc Natl Acad Sci USA* 1998;**95**:2979–2984.
41. Rubart M, Field LJ. ES cells for troubled hearts. *Nat Biotechnol* 2007;**25**:993–994.
42. Leckband D, Sivasankar S. Cadherin recognition and adhesion. *Curr Opin Cell Biol* 2012;**24**:620–627.
43. Ross RS. The extracellular connections: the role of integrins in myocardial remodeling. *J Card Fail* 2002;**8**:S326–S331.
44. Lee EJ, Choi EK, Kang SK, Kim GH, Park JY, Kang HJ, Lee SW, Kim KH, Kwon JS, Lee KH, Ahn Y, Lee HJ, Cho HJ, Choi SJ, Oh WI, Park YB, Kim HS. N-cadherin determines individual variations in the therapeutic efficacy of human umbilical cord blood-derived mesenchymal stem cells in a rat model of myocardial infarction. *Mol Ther* 2012;**20**:155–167.
45. McCain ML, Parker KK. Mechanotransduction: the role of mechanical stress, myocyte shape, and cytoskeletal architecture on cardiac function. *Pflugers Arch* 2011;**462**:89–104.
46. Kostetskii I, Li J, Xiong Y, Zhou R, Ferrari VA, Patel VV, Molkentin JD, Radice GL. Induced deletion of the N-cadherin gene in the heart leads to dissolution of the intercalated disc structure. *Circ Res* 2005;**96**:346–354.
47. Li J, Patel VV, Kostetskii I, Xiong Y, Chu AF, Jacobson JT, Yu C, Morley GE, Molkentin JD, Radice GL. Cardiac-specific loss of N-cadherin leads to alteration in connexins with conduction slowing and arrhythmogenesis. *Circ Res* 2005;**97**:474–481.
48. de Vries RJ, van Veldhuisen DJ, Dunselman PH. Efficacy and safety of calcium channel blockers in heart failure: focus on recent trials with second-generation dihydropyridines. *Am Heart J* 2000;**139**:185–194.
49. Masumoto A, Mohri M, Shimokawa H, Urakami L, Usui M, Takeshita A. Suppression of coronary artery spasm by the Rho-kinase inhibitor fasudil in patients with vasospastic angina. *Circulation* 2002;**105**:1545–1547.
50. Mohri M, Shimokawa H, Hirakawa Y, Masumoto A, Takeshita A. Rho-kinase inhibition with intracoronary fasudil prevents myocardial ischemia in patients with coronary microvascular spasm. *J Am Coll Cardiol* 2003;**41**:15–19.